Artificial two-phase Nb-Ti nanostructures using powder metallurgy techniques

P. D. Jablonski, P. J. Lee, and D. C. Larbalestier
Department of Materials Science and Engineering, University of Wisconsin-Madison, 1500 Johnson Drive, Madison, Wisconsin 53706

(Received 29 April 1994; accepted for publication 27 May 1994)

Several techniques to form artifical high critical current density superconducting Nb-Ti nanostructures have been reported. A drawback to virtually all of these techniques is that they require fabrication strains of 30 or more to reduce the second phase pinning center to the optimum 1–10 nm size at which critical current densities of 10^3–10^4 A/mm^2 are obtained. Here we describe a powder metallurgy process that yields 6020 A/mm^2 at 2 T and 1470 A/mm^2 at 5 T for an alloy with an upper critical field of ~8 T within the same strain space (~13) employed in the conventional Nb-Ti fabrication process.

Traditional Nb-Ti superconductors can reach critical current density (J_c) values at 5 T, 4.2 K of about 3000–3500 A/mm^2 when the optimized microstructure contains ~20 vol % α-Ti drawn into ribbons 1–2 nm thick. The J_c increases linearly with vol % α-Ti,[1] and no maximum has yet been found. However, the thermodynamics of the system appear to limit the amount of α-Ti to ~20 vol % in the high upper critical field (H_{c_2}) Nb-47 wt %Ti alloy. In order to overcome this volume percent limit for Nb-47 wt %Ti, several investigators[2–9] have introduced the second phase artificially [thus these conductors are described as artificial pinning center (APC) conductors]. In the majority of these conductors, handling considerations require that the second phase be millimeters in diameter at assembly. Unfortunately, this means that the composite requires very large strains (>30) in order to reduce the second phase to a size comparable to the ~5 nm coherence length (ξ). This makes such conductors more difficult to fabricate than conventional conductors for which an extrusion billet diameter of 250–300 mm and a final wire diameter of ~0.75 mm dictates a total composite fabrication strain of order 12. However, if the initial size of the second phase can be reduced to tens of microns, then the strain for an APC conductor is also only on the order of 12. Restricting the fabrication strain to this order has important benefits for conductor yield and fabricability. We report here on a powder metallurgy (PM) process which fulfills this fabrication goal.[10]

Some of the advantages of the process are demonstrated by the fabrication of a composite containing approximately twice the quantity of pinning center which is possible in the conventional process, in this case 40 vol %Nb in a Nb-47 wt %Ti matrix. The Nb powder (45–75 μm diameter) and Nb-47 wt %Ti powder (45–150 μm diameter) were blended and cold isostatically pressed at 50 ksi into a round billet weighing 200 g. This green billet was wrapped in Nb foil and sintered in evacuated quartz for 3 h at 1175 °C, followed by an air cool. The sintered billet was swaged from 15 to 13.7 mm diameter using about 20% reduction in area per pass, after which it was machined to 12.6 mm diameter and cut into four pieces, each about 50 mm long. One of these pieces was canned in copper and warm hydrostatically extruded from 15.9 (ϵ=0) to 5.1 mm diameter. The copper was then dissolved from the core prior to a second heat treatment identical to the first. The primary purpose of the second heat treatment was to dissolve hard impurity particles which caused wire breaks at later stages (see later discussion of Fig. 3). The heat-treated rod was resheathed in copper and drawn into a hexagonal cross section, 1.14 mm diameter flat to flat. 91 pieces 50 mm long were stacked into another copper can and extruded as above to fabricate a multifilament billet, which was then drawn to wires as small as 0.2 mm diameter (ϵ=14).

Refinement of the Nb pinning center microstructure was followed by scanning electron microscopy (SEM) backscatter imaging for strains up to 9.4. Transmission electron microscopy (TEM) was performed on transverse sections from strains of ~10–13. Filament cross-sectional uniformity was evaluated using the methods of High *et al.*[11] on the multifilament composite from extrusion size through final wire size (ϵ~7–14). Vickers hardness was used to follow mechanical strength development in the Nb-Ti. Critical current density was determined using the standard four-point probe method on ~60-cm-long samples with voltage taps 33 cm apart. The resistive transition index n was derived from the voltage-current characteristics ($V \propto I^n$). A resistivity criterion of 1×10^{-14} Ω m was used to determine I_c. The niobium-titanium area was determined by a weigh and etch technique, and the Nb pinning centers were included in the superconducting area.

Figure 1 shows how the Nb pins change shape and size over the strain range of 2.3–5.3. The Nb particles soon develop a ribbon morphology typical of a wire-drawn body-centered cubic metal.[12,13] The average Nb thickness ranged from 12 μm (ϵ=2.3) after extrusion to 1.5 μm (ϵ=5.3), while the filament hardness rose from about 195 kg/mm^2 (ϵ=2.3) to about 225 kg/mm^2 (ϵ=5.3). Upon restacking, extruding, and drawing, the Nb ribbons further thinned to 1–10 nm (Fig. 2), a thickness typical of α-Ti ribbons in optimized conventional Nb-Ti.[14] This microstructural refinement was accomplished with strains of 12–13, thus demonstrating that nanometer scale pins are possible in restricted strain space with the PM APC process.

Wires were tested at diameters of 0.76–0.2 mm (ϵ~11–14), as shown in Fig. 3. J_c increased with strain up to a

 0003-6951/94/65(6)/767/3/$6.00

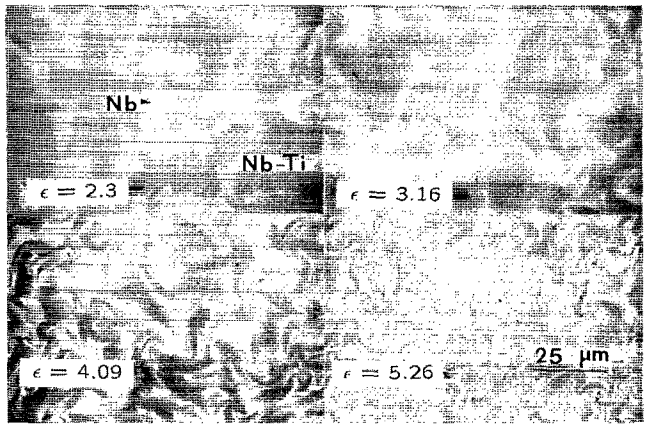

FIG. 1. SEM backscatter electron micrographs showing the typical structure observed in the Nb-Ti filament from post-extrusion (ϵ=2.3) through hexagonal filament stacking size (ϵ=5.3).

maximum at $\epsilon \sim 12.6$. This corresponds to Nb ribbons of a few nanometers in thickness (Fig. 2) which is of the order of ξ.

The testing was not without difficulties, due to the high critical currents of the larger wire sizes (>300 A at low fields) and the presence of some composite defects, which are indicated by the rapid decline of the resistive transition index (n) with increasing strain. n declined from the high value of ~50 at $\epsilon \sim 11.5$ to ~10 at $\epsilon \sim 13$. The lower values are characteristic of heavily sausaged filaments or other forms of filament damage. In this case the coefficient of variation (COV) of the filament cross section was small, remaining ~0.06 through final size (which is similar to good quality SSC composites[15]). However, serious filament breaks associated with impurity Zr particles were seen. The number of broken filaments increased substantially as the strain increased and correlated with the decline in n values. An examination of additional cross sections of the peak J_c wire also revealed broken filaments, although the majority of cross sections showed no defects, consistent with the small COV values measured. Thus, the peak in J_c vs strain is due to a balance between continued microstructural refinement which tends to increase J_c and increasing filament breakage which tends to reduce the effective superconductor cross section. These breaks and the very high currents of some of the 2 T data points in Fig. 3 explain the much greater scatter of

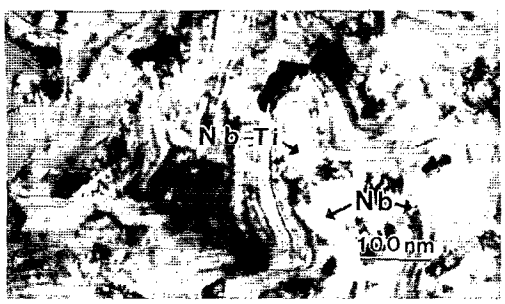

FIG. 2. TEM micrograph showing the pronounced ribbon morphology of the Nb observed at peak J_c size (ϵ=12.6).

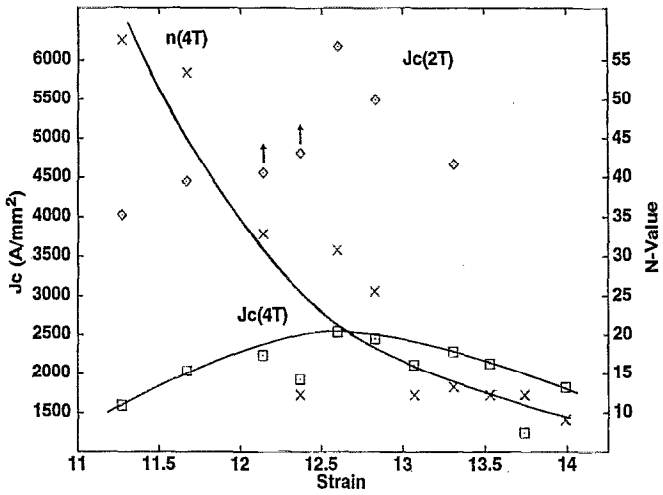

FIG. 3. J_c at 2 and 4 T and n values at 4 T vs strain. No line is drawn for the 2 T data because the two arrowed points quenched erratically below the true J_c.

the 2 T, as compared to the 4 T J_c data points.

An additional factor compromises the high field J_c when this composite is compared to optimized Nb-47 wt %Ti. This is the significantly reduced H_{c_2} of the APC composite, about 7.5 T from the linear extrapolation in Fig. 4, as compared to ~10.7–11 T for Nb–47 wt %Ti. This is a consequence of the overall composition of the wire (60 vol %Nb-47 wt %Ti +40 vol %Nb) being Nb-24 wt %Ti, which is too Nb-rich for maximum H_{c_2}. Given the filament breaks noted above and this reduced H_{c_2}, the attainment of 2500 A/mm^2 at 4 T (~0.5 H_{c_2}) compares very well to maximum values of ~3000 A/mm^2 at 5.5 T (~0.5 H_{c_2}) in Nb-47 wt %Ti.[14,15]

In conclusion, we have demonstrated a new way of fabricating APC composites which develops high J_c values

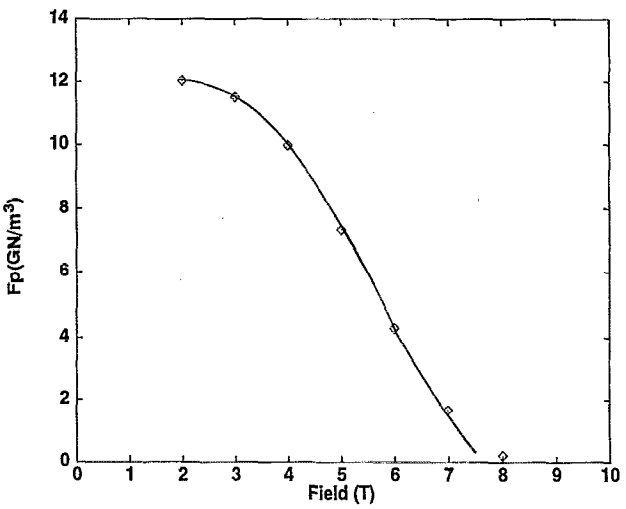

FIG. 4. Flux pinning curve showing the performance at peak J_c size (ϵ =12.6). Note that F_p falls linearly to near zero at about 7.5 T, rather than the expected 11 T value of the Nb-47 wt %Ti matrix. This is a consequence of proximity-induced coupling of the matrix and Nb pins.

from a microstructure which contains substantially more pinning center (~40 vol %) than can be produced by conventional thermal and mechanical processing (~20 vol %). The strain space to produce the nanometer scale flux pinning centers is no larger than for the conventional process. Optimization of the matrix Nb-Ti composition so as to produce an overall composition having optimum H_{c_2} should yield significantly higher J_c values, as should avoidance of impurity contamination in the starting powder.

This work has been supported by the Department of Energy, Division of High Energy Physics.

[1] P. J. Lee, J. C. McKinnell, and D. C. Larbalestier, Adv. Cryo. Eng. (Materials) **36**, 287 (1989).
[2] L. D. Cooley, Ph.D. thesis, U.W.-Madison, 1993.
[3] G. L. Dorofejev, E. Y. Klimenko, S. V. Frolov, E. V. Nikulenkov, E. I. Plashkin, N. I. Salunin, and V. Y. Filkin, in 9th International Conference on Magnet Technology, edited by C. Marinucci and P. Weymuth (Swiss Institute for Nuclear Research, Villigen, Switzerland, 1985), p. 564.
[4] R. M. Scanlan, A. Lietzke, R. Royet, A. Wandesforde, and C. E. Taylor, paper OD-1 presented at Magnet Technology 13, Victoria, BC (1993).
[5] K. Matsumoto, H. Takewaki, Y. Tanaka, O. Miura, K. Yamafuji, K. Funaki, M. Iwakuma, and T. Matsushita, Appl. Phys. Lett. **64**, 115 (1994).
[6] L. Motowidlo, B. Zeitlin, M. Walker, and P. Haldar, Appl. Phys. Lett. **61**, 991 (1994).
[7] J. M. Seuntjens and D. C. Larbalestier, IEEE Trans. **MAG-27**, 1120 (1990).
[8] K. Yamafuji, N. Harada, Y. Mawatari, K. Funaki, T. Matsushita, K. Matsumoto, O. Miura, and Y. Tanaka, Cryogenics **31**, 431 (1991).
[9] B. Zeitlin, M. Walker, and L. Motowidlo, U.S. Patent No. 4,803,310 (February 7, 1989).
[10] P. D. Jablonski and D. C. Larbalestier, U.S. Patent No. 5,226,947 (July 13, 1993).
[11] Y. E. High, P. J. Lee, J. C. McKinnell, and D. C. Larbalestier, Adv. Cry. Eng. (Materials) **38**, 647 (1992).
[12] W. F. Hosford, Jr., Trans. AIME **12**, 12 (1964).
[13] J. C. Malzahn-Kampe and T. H. Courtney, Scripta Met. **23**, 141 (1989).
[14] C. Meingast, P. J. Lee, and D. C. Larbalestier, J. Appl. Phys. **66**, 5962 (1989).
[15] P. J. Lee and D. C. Larbalestier, IEEE Trans. Appl. Suppl. **3**, 833 (1993).